Nonuniversality of heat engine efficiency at maximum power

Sang Hoon Lee,[1,2] Jaegon Um,[3,4,*] and Hyunggyu Park[1,3,†]

[1]*School of Physics, Korea Institute for Advanced Study, Seoul 02455, Korea*
[2]*Department of Liberal Arts, Gyeongnam National University of Science and Technology, Jinju 52725, Korea*
[3]*Quantum Universe Center, Korea Institute for Advanced Study, Seoul 02455, Korea*
[4]*CCSS, CTP and Department of Physics and Astronomy, Seoul National University, Seoul 08826, Korea*

We study the efficiency of a simple quantum dot heat engine at maximum power. In contrast to the quasi-statically operated Carnot engine whose efficiency reaches the theoretical maximum, recent research on more realistic engines operated in a finite time has revealed other classes of efficiencies such as the Curzon-Ahlborn efficiency maximizing the power. Such a power-maximizing efficiency has been argued to be always the half of the maximum efficiency up to the linear order near equilibrium under the tight-coupling condition between thermodynamic fluxes. We show, however, that this universality may break down for the quantum dot heat engine, depending on the constraint imposed on the engine control parameters, even though the tight-coupling condition remains satisfied. It is shown that this deviation is critically related to the applicability of the linear irreversible thermodynamics.

PACS numbers: 05.70.Ln, 05.70.-y, 05.40.a

I. INTRODUCTION

The efficiency of heat engines is a quintessential topic of thermodynamics [1]. In particular, an elegant formula expressed only by hot and cold reservoir temperatures for the ideal quasi-static and reversible engine coined by Sadi Carnot has been an everlasting textbook example [2]. That ideal engine, however, is not the most efficient engine any more when we consider its power output (the extracted work per unit time), which has added different types of optimal engine efficiencies such as the Curzon-Ahlborn (CA) efficiency for some cases [3–5]. Following such steps, researchers have taken simple systems to investigate various theoretical aspects of underlying principles of macroscopic thermodynamic engine efficiency in details [6–14].

In this paper, we take a quantum dot heat engine composed of a single quantum dot connected to two leads with characteristic temperatures and chemical potentials [15–18] to elucidate the condition for the maximum power (Fig. 1). We consider various restricted control-parameter spaces to maximize the power output and find an intriguing result: When the quantum dot energy level relative to one of the lead's chemical potential is fixed and the other is varied, the linear coefficient of the power-maximizing efficiency $\eta_{\rm op}$ near equilibrium takes the conventional CA value of $1/2$, i.e. $\eta_{\rm op} \approx \frac{1}{2}\eta_C$ for small η_C (Carnot efficiency) [13], but its quadratic coefficient deviates from the CA value of $1/8$, which has been already noticed in a previous study [14]. On the other hand, when the quantum dot energy level is varied with fixed chemical potentials of both leads, we find that even the linear coefficient deviates from $1/2$ that has been believed to be "universal" for any tight-coupling engine [13, 14]. In this case, the linear coefficient turns out to be unity ($\eta_{\rm op} \approx \eta_C$), which implies a much higher efficiency at maximum power, compared to the conventional cases.

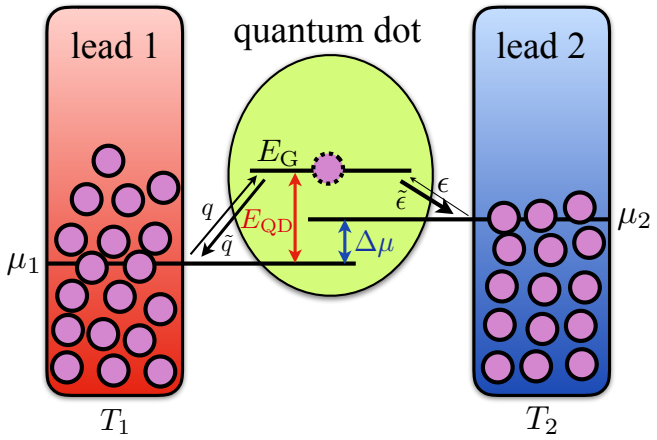

FIG. 1. A schematic illustration of the quantum dot heat engine. The quantum dot with a single energy level $E_{\rm G}$ is in contact with the leads, which plays the role of heat and particle reservoirs with temperatures T_1 and T_2, and chemical potentials μ_1 and μ_2. The maximum (Carnot) efficiency is given as $\eta_C = 1 - T_2/T_1$.

We emphasize that our engine always satisfies the tight-coupling condition in the sense that the heat flux is directly proportional to the work-generating flux [13, 14]. This implies that the universality requires an additional constraint besides the tight-coupling condition, which turns out to be the applicability of the linear irreversible thermodynamics [19]. We point out that the latter non-universal case is also experimentally realizable as it corresponds to tuning the gate voltage of the quantum dot to optimize the power [18], while the control of the chemical potential difference of the leads can be done by adjusting the source-drain voltage [20–23]. In a recent experiment controlling the gate voltage, much higher efficiency than the usual CA efficiency was reported at maximum power [18], which supports our result.

The rest of the paper is organized as follows. We introduce the autonomous quantum dot heat engine model and its mathematically equivalent non-autonomous two-level model

* slung@snu.ac.kr
† hgpark@kias.re.kr

in Sec. II. First, the global optimization of power in the entire parameter space is presented in Sec. III. In Secs. IV and V, we present our main results for the optimization with various constraints and discuss its non-universal feature in power-maximizing efficiency. We conclude with the summary and a remark on future work in Sec. VI.

II. HEAT ENGINE MODELS

A. Quantum dot heat engine model

We take a quantum dot heat engine introduced in Ref. [15], which is composed of a quantum dot whose energy level $E_{\rm G}$ is controlled by the gate voltage where a single electron can occupy, in contact with two leads, denoted by R_1 and R_2 at different temperatures ($T_1 > T_2$) and chemical potentials ($\mu_1 < \mu_2 < E_{\rm G}$), respectively, as shown in Fig. 1. For notational convenience, we define the energy level of the quantum dot as $E_{\rm QD} \equiv E_{\rm G} - \mu_1 > 0$ and the chemical potential difference as $\Delta\mu = \mu_2 - \mu_1 > 0$. Experimentally, it is possible to control $E_{\rm QD}$ by tuning the gate voltage connected to the quantum dot and $\Delta\mu$ by tuning the source-drain voltage connected to the leads [20].

The transition rates of the electron to the quantum dot from R_1 and R_2 are given as the following Arrhenius form,

$$\begin{aligned} q/\tilde{q} &= e^{-E_{\rm QD}/T_1}\,, \\ \epsilon/\tilde{\epsilon} &= e^{-(E_{\rm QD}-\Delta\mu)/T_2}\,, \end{aligned} \tag{1}$$

with q (ϵ) from R_1 (R_2) to the quantum dot and $\tilde{q}$ ($\tilde{\epsilon}$) vice versa. Here, we set the Boltzmann constant $k_B = 1$. Denoting the probability of occupation in the quantum dot by P_o and its complementary probability (of absence) by $P_e = 1 - P_o$, the probability vector $|\mathbf{P}\rangle = (P_o, P_e)^T$ is described by the master equation

$$\frac{d|\mathbf{P}\rangle}{dt} = \begin{pmatrix} -\tilde{q} - \tilde{\epsilon} & q + \epsilon \\ \tilde{q} + \tilde{\epsilon} & -q - \epsilon \end{pmatrix} |\mathbf{P}\rangle\,. \tag{2}$$

For simplicity, tunneling rates between the quantum dot and the leads are chosen as $q + \tilde{q} = \epsilon + \tilde{\epsilon} = 1$. Generalization to arbitrary finite rates does not change our main conclusions. With these normalized rates, we find the condition for parameters as $0 \le \epsilon,\ q \le 1/2$. The steady-state solution is easily obtained as

$$P_{o,ss} = \frac{1}{2}\left(q + \epsilon\right)\,, \quad P_{e,ss} = \frac{1}{2}\left(2 - q - \epsilon\right)\,, \tag{3}$$

with

$$E_{\rm QD} = T_1 \ln\left[\left(1 - q\right)/q\right]\,,\ E_{\rm QD} - \Delta\mu = T_2 \ln\left[\left(1 - \epsilon\right)/\epsilon\right]\,. \tag{4}$$

The probability currents from R_1 to the quantum dot and that from the quantum dot to R_2 are then,

$$\begin{aligned} I_1 &= P_{e,ss} q - P_{o,ss}(1 - q) = \frac{1}{2}(q - \epsilon)\,, \\ I_2 &= P_{o,ss}(1 - \epsilon) - P_{e,ss}\epsilon = \frac{1}{2}(q - \epsilon)\,, \end{aligned} \tag{5}$$

respectively, and they are identical to each other, which represents the conservation of the particle flux. From now on, we denote this steady-state particle flux carrying the energy current by

$$J \equiv \frac{1}{2}(q - \epsilon)\,. \tag{6}$$

The heat production rate to the quantum dot from R_1 and that from the quantum dot to R_2 are

$$\begin{aligned} \dot{Q}_1 &= J E_{\rm QD}\,, \\ \dot{Q}_2 &= J\left(E_{\rm QD} - \Delta\mu\right)\,. \end{aligned} \tag{7}$$

A particle moving from the hot lead R_1 to the cold lead R_2 gains the energy $\Delta\mu$, which can be used later as work against an external device. Thus, the *idealized* power of the engine is defined as

$$\dot{W} = \dot{Q}_1 - \dot{Q}_2 = J\Delta\mu\,, \tag{8}$$

by the first law of thermodynamics. With $\Delta\mu > 0$, we need the condition of $q \ge \epsilon$ (non-negative J) for a proper heat engine. It is clear that the tight coupling condition is satisfied in our model because the heat currents are proportional to the work current with proportionality constants given by the non-vanishing ratio of energy control parameters.

The efficiency of the engine is given by the ratio

$$\eta = \frac{\dot{W}}{\dot{Q}_1} = \frac{\Delta\mu}{E_{\rm QD}} = 1 - \frac{T_2 \ln\left[\left(1 - \epsilon\right)/\epsilon\right]}{T_1 \ln\left[\left(1 - q\right)/q\right]}\,, \tag{9}$$

which is independent of temperatures and the particle flux J. By adjusting temperatures to approach the limit of $\epsilon \to q$ from below, η can reach the maximum (Carnot) efficiency [1, 2],

$$\eta_C = 1 - \frac{T_2}{T_1}\,. \tag{10}$$

The total entropy production rate in the steady state is given by the net entropy change rate of the leads;

$$\dot{S} = -\frac{\dot{Q}_1}{T_1} + \frac{\dot{Q}_2}{T_2} \ge 0\,. \tag{11}$$

B. Cyclic two-level heat engine model

The autonomous quantum dot heat engine introduced in Sec. II A is in fact equivalent to a simple non-autonomous cyclic two-level heat engine described in Fig. 2. The two-level system is characterized by two discrete energy states composed of the ground state ($E = 0$) and the excited state ($E = E_1$ or $E = E_2$, depending on the contacting reservoir). The transition rates from the ground state to the excited state are denoted by q and ϵ, respectively, and their reverse processes by $\tilde{q}$ and $\tilde{\epsilon}$. We assume $E_1 > E_2$ and $T_1 > T_2$.

The system is attached to two different reservoirs: R_1 with temperature T_1 during time τ_1, and R_2 with temperature T_2 during time τ_2, and the adiabatic work extraction and insertion

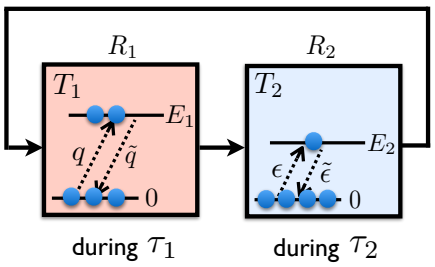

FIG. 2. Schematic illustration of a simple two-level heat engine, composed of two energy levels coupled with two heat reservoirs R_1 and R_2.

occur in between. Although the amount of energy unit involving the work exchange is the same $(E_1 - E_2)$, the net positive work is achievable due to the difference in the population of the excited states at the end of contact with R_1 and R_2, which is determined by model parameters. Then, the mathematical formulation is exactly the same as the quantum dot engine if we use the following mapping from the energy variables in the quantum dot engine in Sec. II A:

$$E_1 \equiv E_{\rm QD}\,, \quad E_2 \equiv E_{\rm QD} - \Delta\mu\,. \tag{12}$$

Using the same formalism as in the autonomous quantum dot engine except for the explicit time dependence, the net work per cycle (cyclic period $\tau = \tau_1 + \tau_2$) in the cyclic steady state is given as

$$W_{\rm net,two\text{-}level} = \frac{\left(1 - e^{-\tau/2}\right)^2 (q - \epsilon)}{1 - e^{-\tau}} (E_1 - E_2)\,, \tag{13}$$

assuming $\tau_1 = \tau_2 = \tau/2$ for simplicity. The τ-dependent factor $\left(1 - e^{-\tau/2}\right)^2 / (1 - e^{-\tau})$ is decoupled from the rest of the formula and thus is just an overall factor. The decoupling holds regardless of the $\tau_1 = \tau_2$ condition; the overall factor becomes $(1 - e^{-\tau_1})(1 - e^{-\tau_2}) / \left[1 - e^{-(\tau_1+\tau_2)}\right]$. The mean power is then given by

$$\frac{W_{\rm two\text{-}level}}{\tau} = \frac{\left(1 - e^{-\tau/2}\right)^2 (q - \epsilon)}{\tau\,(1 - e^{-\tau})} (E_1 - E_2)\,, \tag{14}$$

which decreases monotonically with τ.

This result is exactly the same as the power for the quantum dot engine in Eq. (8) by replacing the current J by $J_{\rm cyc} = a(\tau)J$ with $a(\tau) = 2(1 - e^{-\tau/2})^2/[\tau(1 - e^{-\tau})]$. In fact, all formulas for various other quantities are also written with $J_{\rm cyc}$ instead of J, thus the analysis for the quantum dot engine in the following sections should apply to the cyclic two-level heat engine with a trivial overall factor $a(\tau)$.

III. EFFICIENCY AT MAXIMUM POWER: GLOBAL OPTIMIZATION

In this section, we investigate the efficiency at maximum power for the quantum dot engine. We rewrite Eq. (8) for power in terms of q and ϵ as

$$\dot{W}(q, \epsilon) = \frac{1}{2}(q - \epsilon)\left[T_1 \ln\left(\frac{1 - q}{q}\right) - T_2 \ln\left(\frac{1 - \epsilon}{\epsilon}\right)\right]. \tag{15}$$

The condition for a proper heat engine with non-negative power ($\dot{W} \geq 0$) further restricts the parameter space of (q, ϵ) with

$$\frac{1 - q}{q} \leq \frac{1 - \epsilon}{\epsilon} \leq \left(\frac{1 - q}{q}\right)^{T_1/T_2}. \tag{16}$$

Note that the lower bound corresponds to $J = 0$ (the *reversible* limit with $\dot{S} = 0$) and the upper bound corresponds to $\Delta\mu = 0$ (no work limit with $\dot{W} = 0$).

For given T_1 and T_2, the power can be maximized at (q^*, ϵ^*) inside the above restricted parameter space, which satisfies

$$\left.\frac{\partial \dot{W}}{\partial q}\right|_{(q^*,\epsilon^*)} = \left.\frac{\partial \dot{W}}{\partial \epsilon}\right|_{(q^*,\epsilon^*)} = 0\,, \tag{17}$$

(see details in Appendix A). The efficiency at maximum power, $\eta_{\rm op}$, can be obtained from Eq. (9) with (q^*, ϵ^*), which is a function of the temperature ratio $T_2/T_1 (= 1 - \eta_C)$. This function cannot be written in a closed form with η_C, but its expansion near equilibrium (small η_C) is given by

$$\eta_{\rm op} = \frac{1}{2}\eta_C + \frac{1}{8}\eta_C^2 + \frac{7 - 24a_0 + 24a_0^2}{96(1 - 2a_0)^2}\eta_C^3 + O\left(\eta_C^4\right), \tag{18}$$

with $a_0 = q^*|_{\eta_C=0^+} \approx 0.083\,222$, which is the solution of $2/(1 - 2a_0) = \ln[(1 - a_0)/a_0]$. The same expression was reported previously in equivalent models [15, 17].

We can compare $\eta_{\rm op}$ with the conventional Curzon-Ahlborn (CA) efficiency [3–5] as

$$\eta_{\rm CA} = 1 - \sqrt{T_2/T_1} = 1 - \sqrt{1 - \eta_C}\,, \tag{19}$$

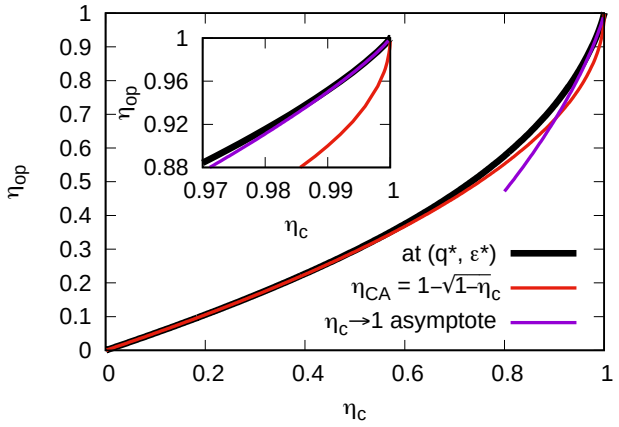

FIG. 3. The efficiency at maximum power $\eta_{\rm op}$ with respect to both q and ϵ versus the Carnot efficiency η_C. The CA efficiency $\eta_{\rm CA}$ in Eq. (19) and and the $\eta_C \to 1$ asymptote in Eq. (21) are also shown. The inset shows the magnified view of the region $0.97 < \eta_C < 1$.

with the expansion form

$$\eta_{\rm CA} = \frac{1}{2}\eta_C + \frac{1}{8}\eta_C^2 + \frac{1}{16}\eta_C^3 + \frac{5}{128}\eta_C^4 + O(\eta_C^5)\,. \qquad (20)$$

The two efficiencies share the same coefficients up to the quadratic terms in the expansion, which are known to be *universal* due to tight-coupling between thermodynamic fluxes and the left-right symmetry [13, 14]. The third order coefficient ($\simeq 0.077\,492$) in Eq. (18), however, is different from $1/16$ ($= 0.0625$) for the $\eta_{\rm CA}$. Plots of $\eta_{\rm op}$ and $\eta_{\rm CA}$ against η_C are shown in Fig. 3 for comparison.

The asymptotic behavior of $\eta_{\rm op}$ near $\eta_C = 1$ is given by

$$\eta_{\rm op} = 1 + (1-b_0)(1-\eta_C)\ln(1-\eta_C) + O\left[(1-\eta_C)\right]\,, \qquad (21)$$

with $b_0 = q^*|_{\eta_C=1^-} \approx 0.217\,812$ which is the solution of $1/(1-b_0) = \ln[(1-b_0)/b_0]$. This result is also shown in Fig. 3 for comparison with $\eta_{\rm CA}$.

IV. LOCAL OPTIMIZATION FOR ONE ENERGY VARIABLE FIXED

For given T_1 and T_2, we fix the quantum dot energy and one of the chemical potential. We vary $\Delta\mu$ (thus ϵ) with fixed $E_{\rm QD}$ (so fixed q).

A. efficiency at maximum power

For given q (or $E_{\rm QD}$), we find ϵ^* maximizing the power in Eq. (15) with $\partial\dot{W}/\partial\epsilon|_{\epsilon^*} = 0$ in the parameter space restricted by Eq. (16). A straightforward calculation similar to the global optimization in Sec. III yields the efficiency at maximum power for small η_C as

$$\eta_{\rm op} = \frac{1}{2}\eta_C + \frac{E_{\rm QD}}{16T_2}\tanh\left(\frac{E_{\rm QD}}{2T_2}\right)\eta_C^2 + O\left(\eta_C^3\right)\,. \qquad (22)$$

The linear coefficient $1/2$ may be regarded as natural due to the tight-coupling condition [13] in our model. More detailed discussion on this $1/2$ universality will be given later in Sec.V B.

The quadratic coefficient is not universal, depending on the system parameter $E_{\rm QD}$, thus differs in general from the universal value $1/8$ representing the left-right symmetry. This implies that the left-right symmetry should be considered not only in the engine device by itself, but also in the allowed parameter space which is broken in this local optimization case. We note that the universal value $1/8$ is recovered for the special case of

$$\frac{E_{\rm QD}}{T_2}\tanh\left(\frac{E_{\rm QD}}{2T_2}\right) = 2\,. \qquad (23)$$

Plots of $\eta_{\rm op}$ against η_C are shown in Fig. 4. It is interesting to note that the asymptotic behavior of $\eta_{\rm op}$ near $\eta_C = 1$ is quite different from that in the case of the global optimization (see Sec. III) and its leading order is given by $\eta_{\rm op} \approx 1 - \alpha_0 + O(1-\eta_C)$ with α_0 satisfying the equation $1 = \alpha_0 + (T_2/E_{\rm QD})\sinh[\alpha_0 E_{\rm QD}/T_2]$. Note that $0 \le \alpha_0 \le 1/2$.

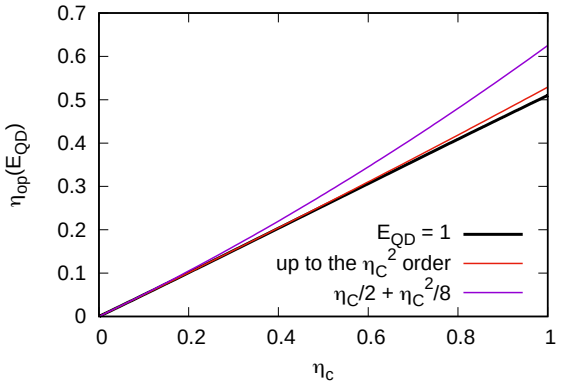

FIG. 4. The efficiency at maximum power $\eta_{\rm op}$ versus η_C for $E_{\rm QD} = 1$ and $T_2 = 1$. The black thick curve represents the exact one. The red thin line is drawn from the expansion in Eq. (22) up to the quadratic order, which is very close to the exact one. For comparison, we also plot the $\eta_C/2 + \eta_C^2/8$ curve (purple thin line), which differs significantly.

B. irreversible thermodynamics approach

Near equilibrium, it is useful to analyze a heat engine in the viewpoint of irreversible thermodynamics [19, 24, 25]. The total entropy production rate in Eq. (11) can be written as

$$\dot{S} = \dot{Q}_1\left(\frac{1}{T_2} - \frac{1}{T_1}\right) - \frac{\dot{W}}{T_2} \equiv J_t X_t + J_1 X_1\,, \qquad (24)$$

with the thermal flux

$$J_t = \dot{Q}_1 = J E_{\rm QD}\,, \qquad (25)$$

the thermal force representing the temperature gradient

$$X_t = \frac{1}{T_2} - \frac{1}{T_1} = \frac{\eta_C}{T_2}\,, \qquad (26)$$

the mechanical flux

$$J_1 = -JT_2\,, \qquad (27)$$

and the mechanical force representing the chemical potential gradient,

$$X_1 = \frac{\Delta\mu}{T_2^2}\,. \qquad (28)$$

Accordingly, the product of mechanical flux and mechanical force leads to the power

$$\dot{W} = J\Delta\mu = -T_2 J_1 X_1\,. \qquad (29)$$

The condition $X_t = X_1 = 0$ corresponds to the thermal and mechanical equilibrium state with $\dot{S} = \dot{W} = 0$.

We expand the particle flux J in Eq. (6) for small forces X_t and X_1 (small η_C and $\Delta\mu$) and find, after some algebra,

$$J_1 = L(X_1 + \xi X_t)\left[1 + \gamma(X_1 - \xi X_t)\right] + O\left(X_t^3, X_1^3\right) \qquad (30)$$

$$J_t = \xi J_1\,, \qquad (31)$$

where

$$L = \frac{T_2^2 e^{-E_{\rm QD}/T_2}}{2\left(1+e^{-E_{\rm QD}/T_2}\right)^2}\,, \xi = -\frac{E_{\rm QD}}{T_2}\,, \gamma = \left(\frac{T_2}{2}\right)\tanh\left(\frac{E_{\rm QD}}{2T_2}\right). \tag{32}$$

Eq. (31) indicates that the tight-coupling condition is satisfied [13].

We optimize power in Eq. (29) with respect to X_1 and find the optimal X_1^* up to the quadratic order of X_t as

$$X_1^* = -\frac{\xi}{2}X_t + \frac{\gamma\xi^2}{8}X_t^2\,. \tag{33}$$

Since the efficiency is given by

$$\eta = \frac{\dot{W}}{\dot{Q}_1} = -\frac{J_1 X_1 T_2}{J_t} = -\frac{X_1 T_2}{\xi}\,, \tag{34}$$

the efficiency at maximum power is obtained as

$$\eta_{\rm op} = \frac{1}{2}\eta_C - \frac{\xi\gamma}{8T_2}\eta_C^2 + O\left(\eta_C^3\right)\,, \tag{35}$$

which is obviously the same as that in Eq. (22). The condition of Eq. (23) to get the universal quadratic coefficient $1/8$ is equivalent to the "energy-matching condition" described in Ref. [25].

V. OPTIMIZATION FOR CHEMICAL POTENTIAL DIFFERENCE FIXED

For given T_1 and T_2, we fix both chemical potentials and vary $E_{\rm QD}$ to find the power maximum. This situation is natural and easily realizable experimentally for a quantum dot engine where the source-drain voltage is fixed, while the gate voltage is adjusted to maximize the power [20–23]. It is in contrast to the previous cases where the maximum power is obtained by adjusting either or both of the source-drain voltages.

A. efficiency at maximum power

It is convenient to rewrite the expression for power in Eqs. (8) and (15) in terms of energy variables $\Delta\mu$ and $E_{\rm QD}$ as

$$\dot{W} = \frac{1}{2}\left(\frac{e^{-E_{\rm QD}/T_1}}{1+e^{-E_{\rm QD}/T_1}} - \frac{e^{-E_{\rm QD}/T_2}e^{\Delta\mu/T_2}}{1+e^{-E_{\rm QD}/T_2}e^{\Delta\mu/T_2}}\right)\Delta\mu\,. \tag{36}$$

For fixed $\Delta\mu > 0$, $\dot{W}$ varies with $E_{\rm QD}$ in the parameter range of $E_{\rm QD} \geq \Delta\mu/\eta_C$ ($q \geq \epsilon$). Note that the boundary point $E_{\rm QD}^r = \Delta\mu/\eta_C$ is a reversible one, where $\dot{W} = \dot{S} = 0$ along with $\eta = \eta_C$.

As $E_{\rm QD}$ increases from the reversible point, $\dot{W}$ increases first but should decrease later after an optimal point because Eq. (36) indicates that $\dot{W}$ should vanish as $E_{\rm QD} \to \infty$. The asymptotic point ($E_{\rm QD} = \infty$) is special with the particle current $J = 0$ in Eq.(6) but $q/\epsilon = e^{-\Delta\mu/T_2} \neq 1$ (broken detailed balance). The optimal point with maximum power is obtained by

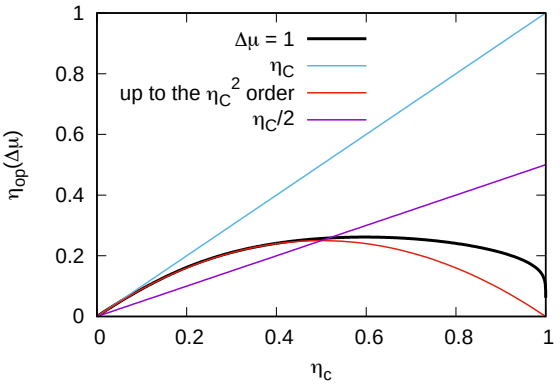

FIG. 5. The efficiency at maximum power $\eta_{\rm op}$ for $\Delta\mu = 1$ and $T_2 = 1$. The black thick curve represents the exact one. It clearly shows that the slope for small η_C is 1, rather than $\frac{1}{2}$. The red thin line is drawn from the expansion in Eq. (40) up to the quadratic order, which is very close to the exact one up to $\eta_C \approx 0.4$.

$$\left.\frac{\partial\dot{W}}{\partial E_{\rm QD}}\right|_{E_{\rm QD}=E_{\rm QD}^*} = 0\,, \tag{37}$$

where the optimal $E_{\rm QD}^*$ satisfies

$$\frac{e^{-E_{\rm QD}^*/T_1}}{\left(1+e^{-E_{\rm QD}^*/T_1}\right)^2}\frac{T_2}{T_1} = \frac{e^{-E_{\rm QD}^*/T_2}e^{\Delta\mu/T_2}}{\left(1+e^{-E_{\rm QD}^*/T_2}e^{\Delta\mu/T_2}\right)^2}\,. \tag{38}$$

First, consider the asymptotic behavior near small η_C. The reversible point $E_{\rm QD}^r = \Delta\mu/\eta_C$ diverges as well as the optimal point $E_{\rm QD}^*$. Keeping the lowest order terms of $e^{-E_{\rm QD}^*/T_2}$ in Eq. (38), we easily obtain

$$E_{\rm QD}^* = \frac{\Delta\mu}{\eta_C} - \frac{T_2}{\eta_C}\ln\left(1-\eta_C\right). \tag{39}$$

Inserting this into Eq. (9), we finally arrive at the efficiency at maximum power as

$$\eta_{\rm op} = \eta_C - \frac{T_2}{\Delta\mu}\eta_C^2 + O\left(\eta_C^3\right)\,. \tag{40}$$

In contrast to the previous cases, the linear coefficient in the expansion deviates from the $1/2$ universality and becomes unity along with the negative quadratic coefficient. This example clearly illustrates that this seemingly robust universality for conventional tight-coupling engines [13] can be also violated, depending on the type of restricted control-parameter spaces used in the power maximization. In the next subsection, we will discuss about the violation of the $1/2$ universality in the perspective of irreversible thermodynamics and the singular behaviors of thermodynamic and mechanical fluxes.

Next, we consider near $\eta_C \approx 1$. In Fig. 5 where the exact result (numerically obtained) is displayed for all values of η_C, we note that $\eta_{\rm op}$ does not increase monotonically

with η_C and vanishes at $\eta_C = 1$ with a singularity. After some algebra, we find indeed a logarithmic singularity such as $\eta_{\rm op} \approx (\Delta\mu/T_2)/[-\ln(1-\eta_C)]$.

B. irreversible thermodynamics approach

As $E_{\rm QD}$ is varied with fixed $\Delta\mu$, the mechanical force X_1 in Eq. (28) cannot be used as a mechanical force variable. Instead, we take the mechanical force defined as

$$X_2 = \frac{1}{E_{\rm QD}} \tag{41}$$

and the corresponding mechanical flux J_2 should be given as

$$J_2 = -\frac{\dot{W}}{T_2 X_2} = -J\frac{\Delta\mu}{T_2}E_{\rm QD}\,. \tag{42}$$

Then, we write the entropy production rate in the standard form as

$$\dot{S} = J_t X_t + J_2 X_2\,, \tag{43}$$

with the same thermal flux $J_t = JE_{\rm QD}$ and force $X_t = \eta_C/T_2$ in Eqs. (25) and (26).

In contrast to the previous case with fixed $E_{\rm QD}$ in Sec. IV, the condition $X_t = X_2 = 0$ does *not* correspond to equilibrium because of non-zero $\Delta\mu$. At the $X_2 = 0$ ($E_{\rm QD} = \infty$) point, the particle current J vanishes (exponentially) as well as $\dot{Q}_1 = \dot{W} = 0$ with $\eta = \Delta\mu/E_{\rm QD} = 0$ (see Eq. (9)). As mentioned in the previous subsection, the detailed balance is broken due to $q/\epsilon \neq 1$. Even though $\dot{S} = 0$ at this point, the average entropy production per one particle transfer diverges as $\dot{S}/J \approx E_{\rm QD}\eta_C/T_2$, which reveals its *irreversible* feature. (A similar situation was discussed in [26].) Therefore, although our approach is dealing with vanishing fluxes in the limit of $X_t \to 0$ and $X_2 \to 0$, it is not technically the conventional irreversible thermodynamics used in Refs. [19, 24, 25], which is a perturbation theory based on the true equilibrium state. Nevertheless, in the following, we present the same type of irreversible thermodynamics analysis and its implication for better understanding of the situation.

Let us start with the tight-coupling condition between J_t and J_2,

$$J_t/J_2 = -T_2/\Delta\mu \equiv \xi'\,, \tag{44}$$

which is a constant in the optimization process in this section. This condition guarantees that the reversible condition $\dot{S} = 0$ can be achieved at non-zero forces with $X_2 = -\xi' X_t$, similar to the standard irreversible thermodynamics discussed in Sec. IV B. Expansion of the mechanical flux in Eq. (42) for small forces X_t and X_2 leads to

$$J_2 = \frac{\Delta\mu}{2T_2X_2}e^{-\frac{1}{T_2X_2}}\left(e^{\Delta\mu/T_2} - e^{X_t/X_2}\right) + O\left(e^{-\frac{2}{T_2X_2}}, e^{\frac{2(T_2X_t-1)}{T_2X_2}}\right), \tag{45}$$

which vanishes as $X_2 \sim X_t \to 0$ with an *essential* singularity rather than linearly seen in Sec. IV B. This implies that the *linear* irreversible thermodynamic analysis is not applicable to our case.

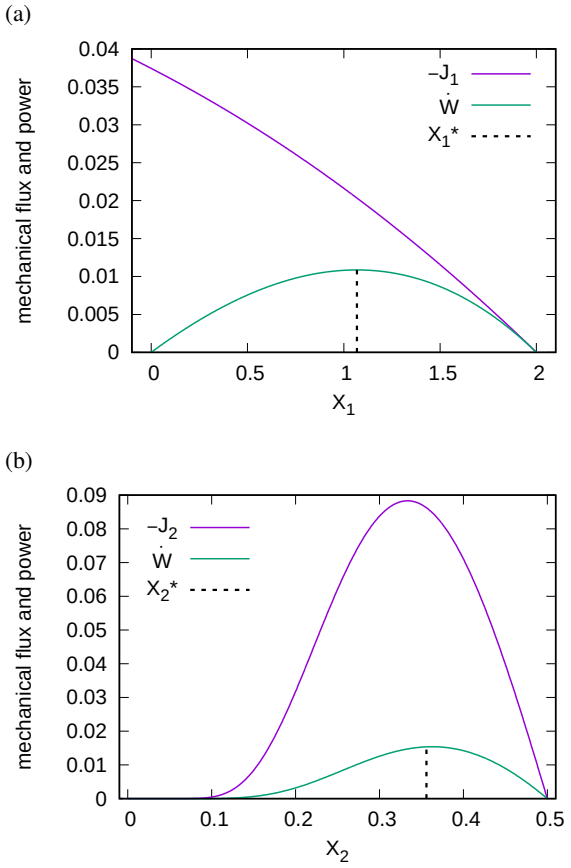

FIG. 6. Comparison between (a) the fixed-$E_{\rm QD}$ case and (b) the fixed-$\Delta\mu$ case, in terms of the mechanical flux (we plot the negative value of the flux for better visualization) and power, where we set $T_1 = 1$ and $T_2 = 1/2$. In (a), we plot J_1 and $\dot{W}$ against the mechanical force X_1 at $E_{\rm QD} = 1$. Both J_1 and $\dot{W}$ vanish at $X_1 = -\xi X_t = E_{\rm QD}\eta_C/T_2^2 = 2$, but only $\dot{W}$ vanishes at $X_1 = 0$. In (b), we plot J_2 and $\dot{W}$ against X_2 at $\Delta\mu = 1$. In this case, both J_2 and $\dot{W}$ vanish at both $X_2 = -\xi' X_t = \eta_C/\Delta\mu = 1/2$ and $X_2 = 0$. For each case, we indicate the optimal values of X_1^* and X_2^* at maximum power.

Plots of the power $\dot{W}$ and the mechanical flux J_1 for the fixed-$E_{\rm QD}$ case in Sec.IV A and J_2 for the fixed-$\Delta\mu$ case in this section are shown for comparison in Fig. 6. For the fixed-$E_{\rm QD}$ case shown in Fig. 6(a), $\dot{W}$ should be approximated as a simple parabola for very small η_C (thus very small parameter interval), because the limiting behaviors near both boundaries ($X_1 = 0$ and $X_1 = -\xi X_t$) are linear, which is usually the case in most optimization procedures. Then the optimal X_1^* is right at the middle point ($X_1^* = -\xi X_t/2$). On the other hand, the efficiency increases linearly such as $\eta = \Delta\mu/E_{\rm QD} \sim X_1$ and reaches η_C at the reversible point ($X_1 = -\xi X_t$). Thus we can easily expect the $1/2$ universality ($\eta_{\rm op} \simeq \eta_C/2$) at maximum power, in general.

However, for the fixed-$\Delta\mu$ case, the functional behavior of $\dot{W}$ near $X_2 = 0$ is anomalous with an essential singularity, seen in Eq. (45) and in Fig. 6(b). When the parameter inter-

val becomes very small (small η_C), one can easily expect the optimal X_2^* should approach the reversible point $X_2 = -\xi' X_t$, leading to $\eta_{\rm op} \simeq \eta_C$ found in Eq. (40).

For simple analysis, we consider a nonlinear leading term of an arbitrary order in the mechanical flux as

$$J_2 = L' \left(X_2 + \xi' X_t\right) X_2^n \,, \tag{46}$$

which vanishes at the reversible point $X_2 = -\xi' X_t$ and also at $X_2 = X_t = 0$. We optimize the power $\dot{W} = -T_2 J_2 X_2$ in Eq. (42) with respect to X_2 and find the optimal X_2^* by

$$X_2^* = -\frac{n+1}{n+2}\xi' X_t \,, \tag{47}$$

and the efficiency at maximum power is obtained as

$$\eta_{\rm op} = \frac{n+1}{n+2}\eta_C \,. \tag{48}$$

The linear case ($n = 0$) yields $\eta_{\rm op} = \eta_C/2$ for the tight-coupling heat engine [13] as expected. However, our case with an essential singularity in Eq. (45) corresponds to the $n \to \infty$ limit, leading to $\eta_{\rm op} \simeq \eta_C$, which is consistent with our result in Eq. (40), up to the leading order. We remark that our heat engine provides only three possible values of the linear coefficient as 1/2, 1, and 0 (varying $E_{\rm QD}$ and $\Delta\mu$ together such as $\eta_C E_{\rm QD} = \Delta\mu + bT_2$ with $b > 0$).

C. Practical gain of the optimization with chemical potential difference fixed

The effectiveness of an engine should be featured by a high efficiency and a high power output. However, there is a trade-off relation between the power and the efficiency [12], which does not allow both merits simultaneously. In previous subsections, we show that, for small η_C (more realistic situations), the power optimization with fixed $\Delta\mu$ provides us a higher efficiency at maximum power than that in the global optimization discussed in Sec. III. But it is also obvious that its power output cannot be larger than that at the global maximum.

The efficiencies at maximum power $\eta_{\rm op}$ in two local optimizations are shown in Fig. 7(a) in comparison with that in the global optimization. As expected, $\eta_{\rm op}$ for the fixed-$\Delta\mu$ case is larger than that for the global optimization for a rather wide range of η_C ($\eta_C \lesssim 0.5$). We also plot the maximum power in local optimizations scaled by the global optimum value Fig. 7(b). We note that the maximum power for the fixed-$\Delta\mu$ case reaches up to a significant fraction of the global optimum value. For example, the case of $\Delta\mu = 1$ at $\eta_C \simeq 0.3$ gives about 30% larger $\eta_{\rm op}$ than that for the global optimization case and reaches about 70% of the global maximum power [27]. This engine at these parameter values may be viewed as "more effective" than the globally optimized engine in some specific situations preferring a good efficiency.

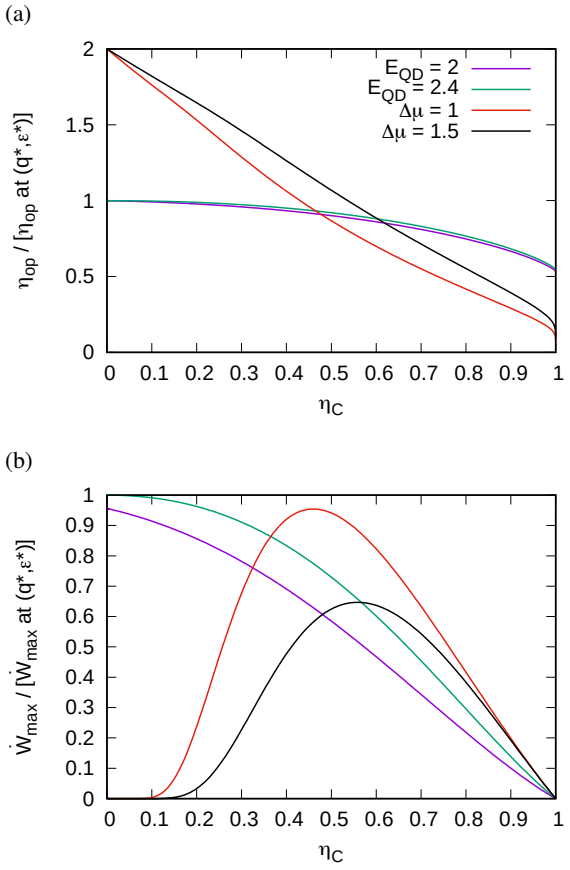

FIG. 7. Comparison between local and global optimizations. (a) The efficiency at maximum power and (b) the maximum power in local optimizations scaled by those in global optimizations with $T_2 = 1$. The purple and green curves correspond to the fixed-$E_{\rm QD}$ case with $E_{\rm QD} = 2$ and 2.4. The red and black curves correspond to the fixed-$\Delta\mu$ case with $\Delta\mu = 1$ and 1.5.

VI. CONCLUSIONS AND DISCUSSION

We have demonstrated that a quantum dot heat engine exhibits various nonuniversal forms of the efficiency at maximum power $\eta_{\rm op}$. In particular, compared to the global or local optimization with varying source-drain voltages, the single-parameter optimization by controlling the gate voltage of the quantum dot for fixed source-drain voltages reveals $\eta_{\rm op} \approx \eta_C$ for small η_C, which breaks the so-called 1/2 universality ($\eta_{\rm op} \approx \frac{1}{2}\eta_C$). This universality has been believed to be robust for any engine with the tight-coupling condition of thermodynamics fluxes.

We have investigated the origin of this universality break down in terms of irreversible thermodynamics and a singular behavior of the mechanical current. In fact, the absence of linear response regime of thermodynamic fluxes may yield various values of the linear coefficient in the standpoint of irreversible thermodynamics. Our case turns out to be an extreme case with an essential singularity in the mechanical current, which makes the efficiency at maximum power close to the Carnot efficiency. A recent experimental study for a quantum dot system [18] shows results consistent with our theoretical finding.

The two mathematically identical two-level heat engine models (autonomous engine and non-autonomous cyclic en-

gine) introduced in Sec. II would naturally involve quantum effects in reality when we take atomic-scale systems. A direction for future works would be taking into account the genuine quantum effects [28–30]. It would be also interesting to study the equivalence of the autonomous and non-autonomous models at the quantum level [30].

ACKNOWLEDGMENTS

We thank Hyun-Myung Chun, Jae Dong Noh, Hee Joon Jeon, and Sang Wook Kim for fruitful discussions and comments. This research was supported by the NRF Grant No. NRF-2017R1D1A1B03030872 (JU) and 2017R1D1A1B06035497 (HP), and by the Gyeongnam National University of Science and Technology Grant in 2018–2019 (SHL).

Appendix A: Global optimization

The global optimization condition, Eq. (17), leads to

$$1-\frac{T_2\ln\left[(1-\epsilon^*)/\epsilon^*\right]}{T_1\ln\left[(1-q^*)/q^*\right]}=\frac{q^*-\epsilon^*}{q^*(1-q^*)\ln\left[(1-q^*)/q^*\right]}\,, \tag{A1a}$$

and

$$1-\frac{T_2\ln\left[(1-\epsilon^*)/\epsilon^*\right]}{T_1\ln\left[(1-q^*)/q^*\right]}=\frac{(T_2/T_1)(q^*-\epsilon^*)}{\epsilon^*(1-\epsilon^*)\ln\left[(1-q^*)/q^*\right]}\,. \tag{A1b}$$

By eliminating the left-hand side of Eqs. (A1a) and (A1b), we obtain the following simple relation

$$\frac{T_2q^*(1-q^*)}{T_1\epsilon^*(1-\epsilon^*)}=1\,, \tag{A2a}$$

or

$$\epsilon^*=\frac{1}{2}\left[1-U(\eta_C,q^*)\right]\,, \tag{A2b}$$

with

$$U(\eta_C,q^*)\equiv\sqrt{4\eta_Cq^*(1-q^*)+(1-2q^*)^2}\,. \tag{A3}$$

By substituting ϵ^* as a function of q^* in Eq. (A2b) to Eq. (A1a) or Eq. (A1b), we get the optimum condition

$$\ln\left(\frac{1-q^*}{q^*}\right)-\frac{T_2}{T_1}\ln\left[\frac{1+U(\eta_C,q^*)}{1-U(\eta_C,q^*)}\right]=\frac{q^*-\frac{1}{2}+\frac{1}{2}U(\eta_C,q^*)}{q^*(1-q^*)}\,. \tag{A4}$$

Furthermore, the condition in Eq. (A4) leads to the following form of $\eta_{\rm op}$ from Eq. (9),

$$\eta_{\rm op}=\frac{q^*-\frac{1}{2}+\frac{1}{2}U(\eta_C,q^*)}{q^*(1-q^*)\ln[(1-q^*)/q^*]}\,. \tag{A5}$$

In order to calculate the efficiency at maximum power for given T_2/T_1, first find the q^* value satisfying Eq. (A4) and substitute the q^* value to Eq. (A5). As Eq. (A4) is a transcendental equation, the closed-form solution for $\eta_{\rm op}$ is not possible in general.

We study analytically asymptotic behaviors of $\eta_{\rm op}$ near $\eta_C=0$ and $\eta_C=1$. First, examine the case for small η_C, using the series expansion of q^* with respect to η_C as

$$q^*=a_0+a_1\eta_C+a_2\eta_C^2+a_3\eta_C^3+O\left(\eta_C^4\right)\,. \tag{A6}$$

Substituting Eq. (A6) into Eq. (A4) and expanding the equation with respect to η_C again, we obtain

$$c_1\eta_C+c_2\eta_C^2+c_3\eta_C^3+O\left(\eta_C^4\right)=0\,, \tag{A7}$$

where c_n is a function of a set of coefficients $\{a_0,\cdots,a_{n-1}\}$. To satisfy Eq. (A7), each c_n should be identically zero. From $c_1=0$, we can easily find

$$\frac{2}{1-2a_0}=\ln\left(\frac{1-a_0}{a_0}\right)\,, \tag{A8}$$

from which we get $a_0\approx 0.083\,222$. This serves as the lower bound of q^*. From $c_2=0$ and $c_3=0$, we can express a_1 and a_2 in terms of a_0. From Eq. (A2b), we can also find ϵ^* as $\epsilon^*=q^*-[a_0(1-a_0)/(1-2a_0)]\eta_C+\cdots$.

With the relations of coefficients in hand, we find the asymptotic behavior of $\eta_{\rm op}$ in Eq. (A5) by expanding it with respect to η_C after substituting q^* as the series expansion of η_C in Eq. (A6). Then, we obtain the expression in Eq. (18) in the main text,

$$\eta_{\rm op}=\frac{1}{2}\eta_C+\frac{1}{8}\eta_C^2+\frac{7-24a_0+24a_0^2}{96(1-2a_0)^2}\eta_C^3+O\left(\eta_C^4\right)\,. \tag{A9}$$

With this method, we are able to find the coefficients in terms of a_0 up to an arbitrary order in principle.

For $\eta_C\simeq 1$, we need to take into account a logarithmic singularity, arising from $\ln[1-U(\eta_C,q^*)]\sim\ln(1-\eta_C)$ in Eq. (A4). We take a singular series expansion of q^* with respect to $1-\eta_C$ as

$$q^*=b_0+b_1'(1-\eta_C)\ln(1-\eta_C)+b_1(1-\eta_C)+O\left[(1-\eta_C)^2\right]\,. \tag{A10}$$

Substituting Eq. (A10) into Eq. (A4) and expanding the equation with respect to $1-\eta_C$, we can identify the equation for b_0 as

$$\frac{1}{1-b_0}=\ln\left(\frac{1-b_0}{b_0}\right)\,, \tag{A11}$$

from which we get $b_0\approx 0.217\,812$. This serves as the upper bound of q^*. We also find $b_1'=b_0(1-b_0)^2$ and $b_1=b_0(1-b_0)^2(1+\ln[b_0(1-b_0)])$. Putting all these together into Eq. (A5), we obtain

$$\begin{aligned}\eta_{\rm op}=&1+(1-b_0)(1-\eta_C)\ln(1-\eta_C)\\&+(1-b_0)\ln[b_0(1-b_0)](1-\eta_C)+O\left[(1-\eta_C)^2\right]\,.\end{aligned} \tag{A12}$$

[1] K. Huang, *Statistical Mechanics* (John Wiley & Sons, New York, 1963).

[2] S. Carnot, *Réflexions Sur La Puissance Motrice Du Feu Et Sur Les Machines Propres À Développer Cette Puissance* (Bachelier Libraire, Paris, 1824).

[3] P. Chambadal, *Les Centrales Nuclaires* (Armand Colin, Paris, 1957).

[4] I. I. Novikov, Efficiency of an atomic power generating installation, At. Energy (N.Y.) **3**, 1269 (1957); The efficiency of atomic power stations, J. Nucl. Energy **7**, 125 (1958).

[5] F. L. Curzon and B. Ahlborn, Efficiency of a Carnot engine at maximum power output, Am. J. Phys. **43**, 22 (1975).

[6] J. Hoppenau, M. Niemann, and A. Engel, Carnot process with a single particle, Phys. Rev. E **87**, 062127 (2013).

[7] K. Proesmans, C. Driesen, B. Cleuren, and C. Van den Broeck, Efficiency of single-particle engines, Phys. Rev. E **92**, 032105 (2015).

[8] J. Um, H. Hinrichsen, C. Kwon, and H. Park, Total cost of operating an information engine, New J. Phys. **17**, 085001 (2015).

[9] V. Holubec and A. Ryabov, Efficiency at and near maximum power of low-dissipation heat engines, Phys. Rev. E **92**, 052125 (2015).

[10] J.-M. Park, H.-M. Chun, and J. D. Noh, Efficiency at maximum power and efficiency fluctuations in a linear Brownian heat engine model, Phys. Rev. E **94**, 012127 (2016).

[11] A. Ryabov and V. Holubec, Maximum efficiency of steady-state heat engines at arbitrary power, Phys. Rev. E **93**, 050101(R) (2016).

[12] N. Shiraishi, K. Saito, and H. Tasaki, Universal trade-off relation between power and efficiency for heat engines, Phys. Rev. Lett. **117**, 190601 (2016).

[13] C. Van den Broeck, Thermodynamic efficiency at maximum power, Phys. Rev. Lett. **95**, 190602 (2005).

[14] M. Esposito, K. Lindenberg, and C. Van den Broeck, Universality of Efficiency at Maximum Power, Phys. Rev. Lett. **102**, 130602 (2009).

[15] M. Esposito, K. Lindenberg, and C. Van den Broeck, Thermoelectric efficiency at maximum power in a quantum dot, Europhys. Lett. **85**, 60010 (2009).

[16] M. Esposito, N. Kumar, K. Lindenberg, and C. Van den Broeck, Stochastically driven single-level quantum dot: A nanoscale finite-time thermodynamic machine and its various operational modes, Phys. Rev. E **85**, 031117 (2012).

[17] R. Toral, C. Van den Broeck, D. Escaff, and K. Lindenberg, Stochastic thermodynamics for Ising chain and symmetric exclusion process, Phys. Rev. E **95**, 032114 (2017).

[18] M. Josefsson, A. Svilans, A. M. Burke, E. A. Hoffmann, S. Fahlvik, C. Thelander, M. Leijnse, and H. Linke, A quantum-dot heat engine operating close to the thermodynamic efficiency limits, Nature Nanotechnology, https://doi.org/10.1038/s41565-018-0200-5 (2018).

[19] S. R. de Groot and P. Mazur, *N*on-Equilibrium Thermodynamics (Dover, New Yor, 1984).

[20] L. P. Kouwenhoven, C. M. Marcus, P. L. McEuen, S. Tarucha, R. M. Westervelt, and N. S. Wingreen, Electron transport in quantum dots, Kluwer Series **E345**, 105–214, in *Proceedings of the NATO Advanced Study Institute on Mesoscopic Electron Transport* (Curaçao, Netherlands Antilles, 1997).

[21] Y. S. Liu, X. F. Yang, X. K. Hong, M. S. Si, F. Chi, and Y. Guo, A high-efficiency double quantum dot heat engine, Appl. Phys. Lett. **103**, 093901 (2013).

[22] T. E. Humphrey, R. Newbury, R. P. Taylor, and H. Linke, Reversible quantum brownian heat engines for electrons, Phys. Rev. Lett. **89**, 116801 (2002).

[23] A. N. Jordan, B. Sothmann, R. Sánchez, and M. Büttiker, Powerful and efficient energy harvester with resonant-tunneling quantum dots, Phys. Rev. B **87**, 075312 (2013).

[24] S. Sheng and Z. C. Tu, Weighted reciprocal of temperature, weighted thermal flux, and their application in finite-time thermodynamics, Phys. Rev. E **89**, 012129 (2014).

[25] S. Sheng and Z. C. Tu, Constitutive relation for nonlinear response and universality of efficiency at maximum power for tight-coupling heat engines, Phys. Rev. E **91**, 022136 (2015).

[26] J. S. Lee and H. Park, Carnot efficiency is attainable in an irreversible process, Sci. Rep. **7**, 10725 (2017).

[27] A similar result was reported experimentally in the lower right panel of Fig. 3(c) in [18], where, with $\eta_C \simeq 0.36$, $\eta_{\rm op}$ is about 25% larger than $\eta_{\rm CA}$ and the power output is about 65% of its global maximum.

[28] H. E. D. Scovil and E. O. Schulz-DuBois, Three-level masers as heat engines, Phys. Rev. Lett. **2**, 262 (1959).

[29] R. Uzdin, Am. Levy, and R. Kosloff, Equivalence of quantum heat machines, and quantum-thermodynamic signatures, Phys. Rev. X **5**, 031044 (2015).

[30] J. Um, K. Dorfman, and H. Park (unpublished).